

1 Functional MRI brain state 2 occupancy in the presence of 3 cerebral small vessel disease – 4 pre-registration for a replication 5 analysis of the Hamburg City Health 6 Study

✉ For correspondence:
e.schlemm@uke.de

Present address:
Dr. Dr. Eckhard Schlemm,
Klinik und Poliklinik für
Neurologie,
Universitätsklinikum
Hamburg-Eppendorf,
Martinistr. 52,
D-20251 Hamburg

Data availability:
Preprocessed data will be
available e.g. on
<https://github.com/csi-hamburg/HCHS-brain-states-RR>.

Funding: Deutsche
Forschungsgemeinschaft
(DFG) - 178316478 - C2

Competing interests: The
author declares no
competing interests.

7 **Eckhard Schlemm, MBBS PhD^①✉ and Thies Ingwersen, MD¹**

8 ¹Department of Neurology, University Medical Center
9 Hamburg-Eppendorf

11 **Abstract**

12 **Objective:** To replicate recent findings about the association between the extent of
13 cerebral small vessel disease (cSVD), functional brain network dedifferentiation and
14 cognitive impairment.
15 **Methods:** We will analyze demographic, imaging and behavioral data from the
16 prospective population-based Hamburg City Health Study. Using a fully prespecified
17 analysis pipeline, we will estimate discrete brain states from structural and resting-state
18 functional magnetic resonance imaging (MRI). In a multiverse analysis we will vary brain
19 parcellations and functional MRI confound regression strategies. Severity of cSVD will
20 be operationalised as the volume of white matter hyperintensities of presumed
21 vascular origin. Processing speed and executive dysfunction are quantified by the trail
22 making test (TMT).
23 **Hypotheses:** We hypothesize a) that greater volume of supratentorial white matter

²⁴ hyperintensities is associated with less time spent in functional MRI-derived brain
²⁵ states of high fractional occupancy; and b) that less time spent in these high-occupancy
²⁶ brain states is associated with longer time to completion in part B of the TMT.

²⁷

²⁸ Introduction

²⁹ Cerebral small vessel disease (cSVD) is an arteriolopathy of the brain, associated with
³⁰ age and common cardiovascular risk factors (Wardlaw, C. Smith, and Dichgans, 2013).
³¹ cSVD predisposes to ischemic, in particular lacunar, stroke and may lead to cognitive im-
³² pairment and dementia (Cannistraro et al., 2019). Neuroimaging findings in cSVD reflect
³³ its underlying pathology (Wardlaw, Valdés Hernández, and Muñoz-Maniega, 2015) and
³⁴ include white matter hyperintensities (WMH) and lacunes of presumed vascular origin,
³⁵ small subcortical infarcts and microbleeds, enlarged perivascular spaces as well as brain
³⁶ atrophy (Wardlaw, E. E. Smith, et al., 2013). However, the extent of visible cSVD features
³⁷ on magnetic resonance imaging (MRI) is an imperfect predictor of the severity of clini-
³⁸ cal sequelae (Das et al., 2019), and our understanding of the causal mechanisms linking
³⁹ cSVD-associated brain damage to clinical deficits remains limited (Bos et al., 2018).

⁴⁰ Recent efforts have concentrated on exploiting network aspects of the structural (Tu-
⁴¹ ladhar, Dijk, et al., 2016; Tuladhar, Tay, et al., 2020; Lawrence, Zeestraten, et al., 2018) and
⁴² functional (Dey et al., 2016; Schulz et al., 2021) organization of the brain to understand
⁴³ the relation between cSVD and clinical deficits in cognition and other domains reliant
⁴⁴ on distributed processing. Reduced structural network efficiency has repeatedly been
⁴⁵ described as a causal factor in the development of cognitive impairment, in particular
⁴⁶ executive dysfunction and reduced processing speed, in cSVD (Lawrence, Chung, et al.,
⁴⁷ 2014; Shen et al., 2020; Reijmer et al., 2016; Prins et al., 2005). Findings with respect to
⁴⁸ functional connectivity (FC), on the other hand, are more heterogeneous than their SC
⁴⁹ counterparts, perhaps because FC measurements are prone to be affected by hemody-
⁵⁰ namic factors and noise, resulting in relatively low reliability, especially with resting-state
⁵¹ scans of short duration (Laumann, Gordon, et al., 2015). This problem is exacerbated
⁵² in the presence of cSVD and made worse by the arbitrary processing choices (Lawrence,
⁵³ Tozer, et al., 2018; Gesierich et al., 2020).

⁵⁴ As a promising new avenue, time-varying, or dynamic, functional connectivity approaches
⁵⁵ have more recently been explored in patients with subcortical ischemic vascular disease

Question	Hypothesis	Sampling plan	Analysis plan	Rationale deciding sensitivity for the test	Interpretation given different outcomes	Theory that could be shown wrong by the outcome
Is severity of cerebral small vessel disease, quantified by the volume of supratentorial white matter hyperintensities of presumed vascular origin (WMH), associated with time spent in high-occupancy brain states, defined by resting-state functional MRI	Higher WMH volume is associated with lower average occupancy of the two highest-occupancy brain states.	Available subjects with clinical and imaging data from the HCHS (Jagodzinski et al., 2020)	Standardized preprocessing of structural and functional MRI data • automatic quantification of WMH • co-activation pattern analysis • multivariable generalised regression analyses	Tradition	$P < 0.05 \rightarrow$ rejection of the null hypothesis of no association between cSVD and fractional occupancy; $P > 0.05 \rightarrow$ insufficient evidence to reject the null hypothesis	Functional brain dynamics are not related to subcortical ischemic vascular disease.

Table 1. Study Design Template

⁵⁶ (Yin et al., 2022; Xu et al., 2021). While the study of dynamic FC measures may not solve
⁵⁷ the problem of limited reliability, especially in small populations or subjects with exten-
⁵⁸ sive structural brain changes, it adds another – temporal – dimension to the study of
⁵⁹ functional brain organisation, which is otherwise overlooked. Importantly, FC dynamics
⁶⁰ do not only reflect moment-to-moment fluctuations in cognitive processes but are also
⁶¹ related to brain plasticity and homeostasis (Laumann and Snyder, 2021; Laumann, Snyder, et al., 2017), which may be impaired in cSVD.

⁶³ In the present paper, we aim to replicate and extend the main results of (Schlemm
⁶⁴ et al., 2022); in this recent study, the authors analyzed MR imaging and clinical data from
⁶⁵ the prospective Hamburg City Health Study (HCHS, (Jagodzinski et al., 2020)) using a coac-
⁶⁶ tivation pattern approach to define discrete brain states and found associations between
⁶⁷ the WMH load, time spent in high-occupancy brain states characterized by activation or
⁶⁸ suppression of the default mode network (DMN) and cognitive impairment.

⁶⁹ The fractional occupancy of a functional MRI-derived discrete brain state is a subject-
⁷⁰ specific measure of brain dynamics defined as the proportion of BOLD volumes assigned
⁷¹ to that state relative to all BOLD volumes acquired during a resting-state scan.

⁷² Our primary hypothesis is that the volume of supratentorial white matter hyperinten-
⁷³ sities is associated with the fractional occupancy of DMN-related brain states in a middle-
⁷⁴ aged to elderly population mildly affected by cSVD. Our second hypothesis is that this
⁷⁵ fractional occupancy is associated with executive dysfunction and reduced processing
⁷⁶ speed, measured as the time to complete part B of the trail making test (TMT).

⁷⁷ Both hypotheses will be tested in an independent subsample of the HCHS study popu-
⁷⁸ lation using the same imaging protocols, examination procedures and analysis pipelines
⁷⁹ as in (Schlemm et al., 2022). The robustness of associations will be explored in a multi-

⁸¹ Methods

⁸² Study population

⁸³ The paper will analyze data from the Hamburg City Health Study (HCHS), which is an
⁸⁴ ongoing prospective, population-based cohort study aiming to recruit a cross-sectional
⁸⁵ sample of 45 000 adult participants from the city of Hamburg, Germany (Jagodzinski et al.,
⁸⁶ 2020). From the first 10 000 participants of the HCHS we will aim to include those who
⁸⁷ were documented to have received brain imaging (n=2652) and exclude those who were
⁸⁸ analyzed in our previous report (Schlemm et al., 2022) (n=988), for an expected sample
⁸⁹ size of approximately 1500 participants. The ethical review board of the Landesärztekam-
⁹⁰ mer Hamburg (State of Hamburg Chamber of Medical Practitioners) approved the HCHS
⁹¹ (PV5131), all participants provided written informed consent.

⁹² Demographic and clinical characterization

⁹³ From the study database we will extract participants' age at the time of inclusion in years,
⁹⁴ their self-reported gender and the number of years spent in education. During the visit
⁹⁵ at the study center, participants undergo cognitive assessment using standardized tests.
⁹⁶ We will extract from the database their performance scores in the Trail Making Test part
⁹⁷ B, measured in seconds, as an operationalization of executive function and psychomotor
⁹⁸ processing speed (Tombaugh, 2004; Arbuthnott and Frank, 2000).

⁹⁹ MRI acquisition and preprocessing

¹⁰⁰ The magnetic resonance imaging protocol for the HCHS includes structural and resting-
¹⁰¹ state functional sequences. The acquisition parameters on a 3 T Siemens Skyra MRI scan-
¹⁰² ner (Siemens, Erlangen, Germany) have been reported before (Petersen et al., 2020; Frey
¹⁰³ et al., 2021) and are given as follows:

¹⁰⁴ For T_1 -weighted anatomical images, a 3D rapid acquisition gradient-echo sequence
¹⁰⁵ (MPRAGE) was used with the following sequence parameters: repetition time TR = 2500 ms,
¹⁰⁶ echo time TE = 2.12 ms, 256 axial slices, slice thickness ST = 0.94 mm, and in-plane resolu-
¹⁰⁷ tion IPR = $(0.83 \times 0.83) \text{ mm}^2$.

¹⁰⁸ T_2 -weighted fluid attenuated inversion recovery (FLAIR) images were acquired with
¹⁰⁹ the following sequence parameters: TR = 4700 ms, TE = 392 ms, 192 axial slices, ST =
¹¹⁰ 0.9 mm, IPR = $(0.75 \times 0.75) \text{ mm}^2$.

¹¹¹ 125 resting state functional MRI volumes were acquired (TR = 2500 ms; TE = 25 ms;

112 flip angle = 90°; slices = 49; ST = 3 mm; slice gap = 0 mm; IPR = (2.66 × 2.66) mm²). Subjects
113 were asked to keep their eyes open and to think of nothing.

114 We will verify the presence and voxel-dimensions of expected MRI data for each par-
115 ticipant and exclude those for whom at least one of T_1 -weighted, FLAIR and resting-state
116 MRI is missing. We will also exclude participants with a neuroradiologically confirmed
117 space-occupying intra-axial lesion. To ensure reproducibility, no visual quality assess-
118 ment on raw images will be performed.

119 For the remaining participants, structural and resting-state functional MRI data will
120 be preprocessed using FreeSurfer v6.0 (<https://surfer.nmr.mgh.harvard.edu/>), and fmriPrep
121 v20.2.6 (Esteban et al., 2019), using default parameters. Participants will be excluded if
122 automated processing using at least one of these packages fails.

123 Quantification of WMH load

124 For our primary analysis, the extent of ischemic white matter disease will be operational-
125 ized as the total volume of supratentorial WMHs obtained from automated segmentation
126 using a combination of anatomical priors, BIANCA (Griffanti, Zamboni, et al., 2016) and
127 LOCATE (Sundaresan et al., 2019), post-processed with a minimum cluster size of 30 vox-
128 ells, as described in (Schlemm et al., 2022). In an exploratory analysis, we partition voxels
129 identified as WMH into deep and periventricular components according to their distance
130 to the ventricular system (cut-off 10 mm, (Griffanti, Jenkinson, et al., 2018))

131 Brain state estimation

132 Output from fMRIprep will be post-processed using xcpEngine v1.2.1 to obtain de-confounded
133 spatially averaged BOLD time series (Ciric, Wolf, et al., 2017). For the primary analysis we
134 will use the 36p regression strategy and the Schaefer-400 parcellation (Schaefer et al.,
135 2018), as in (Schlemm et al., 2022).

136 Different atlases and confound regression strategies, as implemented in xcpEngine,
137 will be included in the exploratory multiverse analysis.

138 Co-activation pattern (CAP) analysis will be performed by first aggregating parcellated,
139 de-confounded BOLD signals into a ($n_{\text{parcels}} \times \sum_i n_{\text{time points},i}$) feature matrix, where $n_{\text{time points},i}$
140 denotes the number of retained volumes for subject i after confound regression. Cluster-
141 ing will be performed using the k -means algorithm ($k = 5$) with distance measure given
142 by 1 minus the sample Pearson correlation between points, as implemented in Matlab
143 R2021a. We will estimate subject- and state-specific fractional occupancies, which are

¹⁴⁴ defined as the proportion of BOLD volumes assigned to each brain state (Vidaurre et al.,
¹⁴⁵ 2018). The two states with the highest average occupancy will be identified as the basis
¹⁴⁶ for further analysis.

¹⁴⁷ Statistical analysis

¹⁴⁸ For demographic (age, gender, years of education) and clinical (TMT-B) variables the num-
¹⁴⁹ ber of missing records will be reported. For non-missing values, we will provide descrip-
¹⁵⁰ tive summary statistics using median and interquartile range. The proportion of men
¹⁵¹ and women in the sample will be reported. Regression modelling will be carried out as
¹⁵² a complete-case analysis.

¹⁵³ As a first outcome-neutral quality check of the implementation of the MRI process-
¹⁵⁴ ing pipeline, brain state estimation and co-activation pattern analysis, we will compare
¹⁵⁵ fractional occupancies between brain states. We expect that the average fractional oc-
¹⁵⁶ cupancy in two high-occupancy states is higher than the average fractional occupancy in
¹⁵⁷ the other three states. Point estimates and 95% confidence intervals will be presented
¹⁵⁸ for the difference in average fractional occupancy to check this assertion.

¹⁵⁹ For further analyses, non-zero WMH volumes will be subjected to a logarithmic trans-
¹⁶⁰ formation. Zero values will retain their value zero; to compensate, all models will include
¹⁶¹ a binary indicator for zero WMH volume if at least one non-zero value is present.

¹⁶² To assess the primary hypothesis of a negative association between the extent of is-
¹⁶³ chemic white matter disease and time spent in high-occupancy brain states, we will per-
¹⁶⁴ form a fixed-dispersion beta-regression to model the logit of the conditional expectation
¹⁶⁵ of the average fractional occupancy of two high-occupancy states as an affine function of
¹⁶⁶ the logarithmized WMH load. Age and gender will be included as covariates. The strength
¹⁶⁷ of the association will be quantified as an odds ratio per interquartile ratio of the WMH
¹⁶⁸ burden distribution and accompanied by a 95% confidence interval. Significance testing
¹⁶⁹ of the null hypothesis of no association will be conducted at the conventional significance
¹⁷⁰ level of 0.05. Estimation and testing will be carried out using the 'betareg' package v3.1.4
¹⁷¹ in R v4.2.1.

¹⁷² To assess the secondary hypothesis of an association between time spent in high-
¹⁷³ occupancy brain states and executive dysfunction, we will perform a generalized linear
¹⁷⁴ regression with a Gamma response distribution to model the logarithm of the condi-
¹⁷⁵ tional expected completion time in part B of the TMT as an affine function of the average
¹⁷⁶ fractional occupancy of two high-occupancy states. Age, gender, years of education and

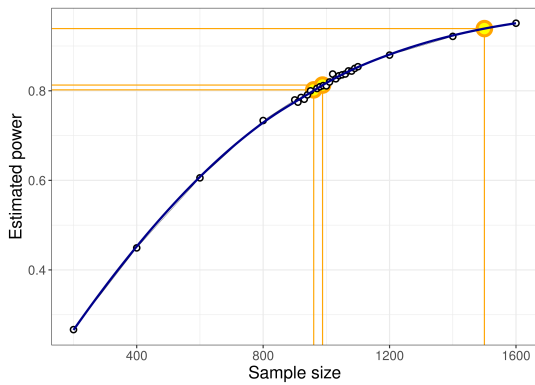


Figure 1. Estimated power for different sample sizes is obtained as the proportion of synthetic data sets in which the null hypothesis of no association between WMH volume and time spent in high-occupancy brain states can be rejected at the $\alpha = 0.05$ significance level. Proportions are based on a total of 10 000 synthetic data sets obtained by bootstrapping the data presented in (Schlemm et al., 2022). Highlighted in orange are the smallest sample size ensuring a power of at least 80 % ($n = 960$), the sample size of the pilot data ($n = 988$, post-hoc power 81.3 %), and the expected sample sample size for this replication study ($n = 1500$, a-priori power 93.9 %).

177 logarithmized WMH load will be included as covariates. The strength of the association
 178 will be quantified as a multiplicative factor per percentage point and accompanied by a
 179 95% confidence interval. Significance testing of the null hypothesis of no association will
 180 be conducted at the conventional significance level of 0.05. Estimation and testing will
 181 be carried out using the `glm` function included in the 'stats' package from R v4.2.1.

182 Sample size calculation is based on an effect size on the odds ratio scale of 0.95, corre-
 183 sponding to an absolute difference in the probability of occupying a DMN-related brain
 184 state between the first and third WMH-load quartile of 1.3 percentage points, and be-
 185 tween the 5% and 95% percentile of 3.1 percentage points. Approximating half the dif-
 186 ference in fractional occupancy of DMN-related states between different task demands
 187 (rest vs n-back) in healthy subjects, which was estimated to lie between 6 and 7 percent-
 188 age points (Cornblath et al., 2020), this value represent a plausible choice for the smallest
 189 effect size of theoretical and practical interest. It also equals the effect size estimated
 190 based on the data presented in (Schlemm et al., 2022).

191 We used simple bootstrapping to create 10 000 hypothetical datasets of size 200, 400,
 192 600, 800, 900, 910, ..., 1100, 1200, 1400, 1500, 1600. Each dataset was subjected to the esti-
 193 mation procedure described above. For each sample size, the proportion of datasets in
 194 which the primary null hypothesis of no association between fractional occupancy and
 195 WMH load could be rejected at $\alpha = 0.05$ was computed and is recorded as a power curve
 196 in Figure 1.

197 It is seen that a sample size of 960 would allow replication of the reported effect with

Name of the atlas	#parcels	Reference	Design	Reference
Desikan-Killiany	86	Desikan et al., 2006	24p	Friston et al., 1996
AAL	116	Tzourio-Mazoyer et al., 2002	24p + GSR	Macey et al., 2004
Harvard-Oxford	112	Makris et al., 2006	36p	Satterthwaite et al., 2013
glasser360	360	Glasser et al., 2016	36p + spike regression	Cox, 1996
gordon333	333	Gordon et al., 2016	36p + despiking	Satterthwaite et al., 2013
power264	264	Power, Cohen, et al., 2011	36p + scrubbing	Power, Mitra, et al., 2014
schaefer{N}	100	Schaefer et al., 2018	aCompCor	Muschelli et al., 2014
	200		tCompCor	Behzadi et al., 2007
	400		AROMA	Pruim et al., 2015

AAL: Automatic Anatomical Labelling

(a) Parcellations

GSR: Global signal regression, AROMA: Automatic Removal of Motion Artifacts

(b) Confound regression strategies, adapted from (Circi, Wolf, et al., 2017)

Table 2. Multiverse analysis, implemented using xcpEngine (Circi, Rosen, et al., 2018)

¹⁹⁸ a power of 80.2 %. We anticipate a sample size of 1500, which yields a power of 93.9 %.

¹⁹⁹ **Multiverse analysis**

²⁰⁰ Both in (Schlemm et al., 2022) and for our primary replication analysis we made certain
²⁰¹ analytical choices in the operationalization of brain states and ischemic white matter
²⁰² disease, namely the use of the *36p* confound regression strategy, the Schaefer-400 par-
²⁰³ cellation and a BIANCA/LOCATE-based WMH segmentation algorithm. The robustness
²⁰⁴ of the association between WMH burden and time spent in high-occupancy states with
²⁰⁵ regard to other choices will be explored in a multiverse analysis (Steegen et al., 2016).
²⁰⁶ Specifically, in an exploratory analysis, we will estimate brain states from BOLD time se-
²⁰⁷ ries processed according to a variety of established confound regression strategies and
²⁰⁸ aggregated over different cortical brain parcellations (Table 2, Circi, Rosen, et al., 2018;
²⁰⁹ Circi, Wolf, et al., 2017). Extent of cSVD will additionally be quantified by the volume of
²¹⁰ deep and periventricular white matter hyperintensities.

²¹¹ For each combination of analytical choice of confound regression strategy, parcella-
²¹² tion and subdivision of white matter lesion load ($9 \times 9 \times 3 = 243$ scenarios in total) we will
²¹³ quantify the association between WMH load and average time spent in high-occupancy
²¹⁴ brain states using odds ratio and 95 % confidence intervals as described above.

²¹⁵ No hypothesis testing and will be carried out in these multiverse analyses. They rather
²¹⁶ serve to inform about the robustness of the outcome of the test of the primary hypothe-
²¹⁷ sis. Any substantial conclusions about the association between severity of cerebral small
²¹⁸ pathology and time spent in high-occupancy brain states, as stated in the Scientific Ques-
²¹⁹ tion in Table 1, will be drawn from the primary analysis using pre-specified methodolog-
²²⁰ ical choices.

221 Further exploratory analysis

222 In previous work, two high-occupancy brain states were related to the default-mode net-
223 work (Cornblath et al., 2020). We will further explore this relation by computing, for each
224 individual brain state, the cosine similarity of the positive and negative activations of
225 the cluster's centroid with a set of a-priori defined functional 'communities' or networks
226 (Schaefer et al., 2018; Yeo et al., 2011). Results will be thus visualized as spider plots for
227 the Schaefer, Gordon and Power atlases.

228 In further exploratory analyses we plan to describe the associations between brain
229 state dynamics and other measures of cognitive ability, such as memory and language.

230 Code and pilot data

231 Summary data from the first 1000 imaging data points of the HCHS have been published
232 with (Schlemm et al., 2022) and form the basis for the hypotheses tested in this replication
233 study. We have implemented our prespecified analysis pipeline described above in R
234 and Matlab, and applied it to this previous sample. Data, code and results have been
235 stored on GitHub (https://github.com/csi-hamburg/HCHS_brain_states_RR) und preserved
236 on Zenodo.

237 Thus re-analysing data from 988 subjects, the separation between two high-occupancy
238 and three low-occupancy brain states could be reproduced for all combinations of brain
239 parcellation and confound regression strategies (Figure 2).

240 In a multiverse analysis, the main finding was somewhat robust with respect to these
241 choices: a statistically significant negative association between WMH load and time spent
242 in high-occupancy states was observed in 18/81 scenarios, with 5/81 statistically signifi-
243 cant positive associations occurring with the Desikan–Killiany parcellation only (Figure 3).

244 The secondary finding of an association between greater TMT-B times and lower frac-
245 tional occupancy was similarly robust with 12/81 statistically significant negative and no
246 statistically significant positive associations.

247 Timeline and access to data

248 At the time of planning of this study, all demographic, clinical and imaging data used in
249 this analysis have been collected by the HCHS and are held in the central trial database.
250 Quality checks for non-imaging variables have been performed centrally. WMH segmen-
251 tation based on structural MRI data of the first 10 000 participants of the HCHS has been

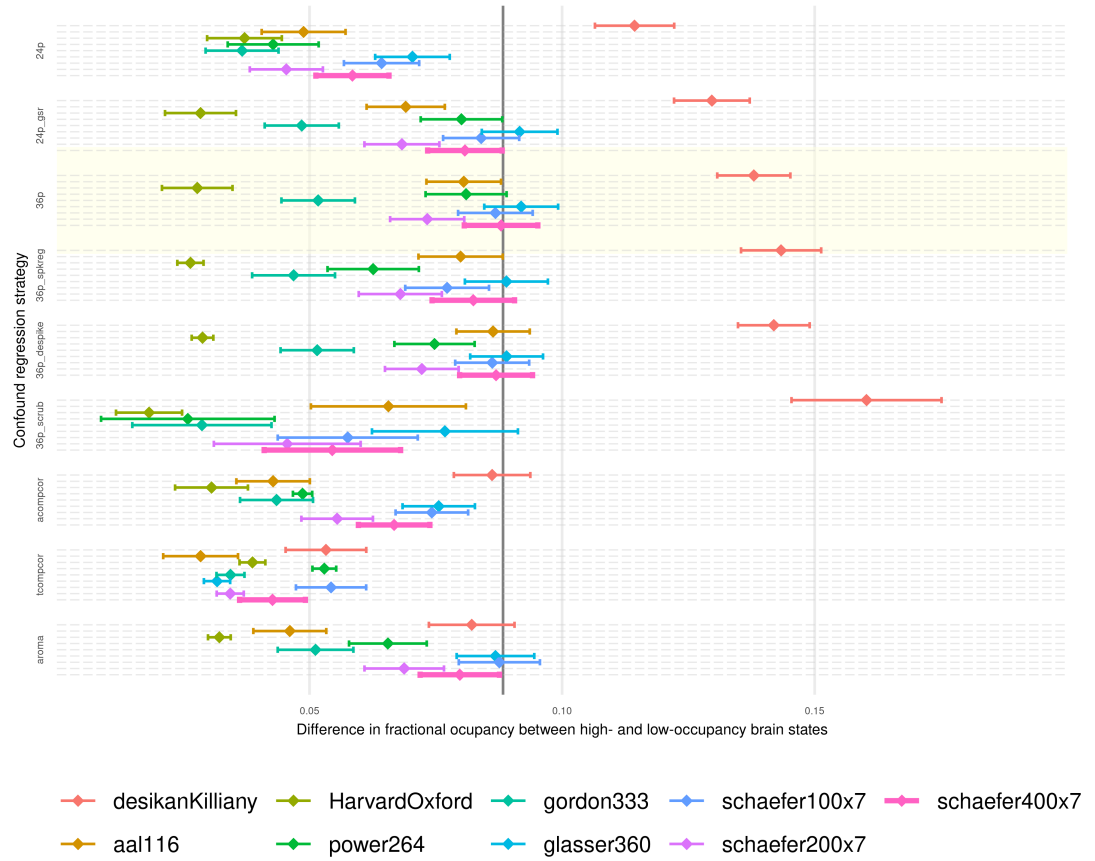


Figure 2. Point estimates (dots) and 95 % confidence intervals (line segments) for the mean difference in fractional occupancy between high- and low occupancy states are shown for different confound regression strategies (groups along the vertical axis) and brain parcellations (color). The difference in FO for a particular choice of regression strategy and brain parcellation is nominally statistically significantly different from zero at a significance level of 5% if the corresponding interval does not contain zero. Hence, the FO difference is significant for *all* processing choices, reflecting the separation between high- und low-occupancy states. The primary choices (36p and schaefer400) are highlighted by a yellow box and thick pink line, respectively. The effect size reported in (Schlemm et al., 2022) is indicated by a vertical line at 0.08830623.

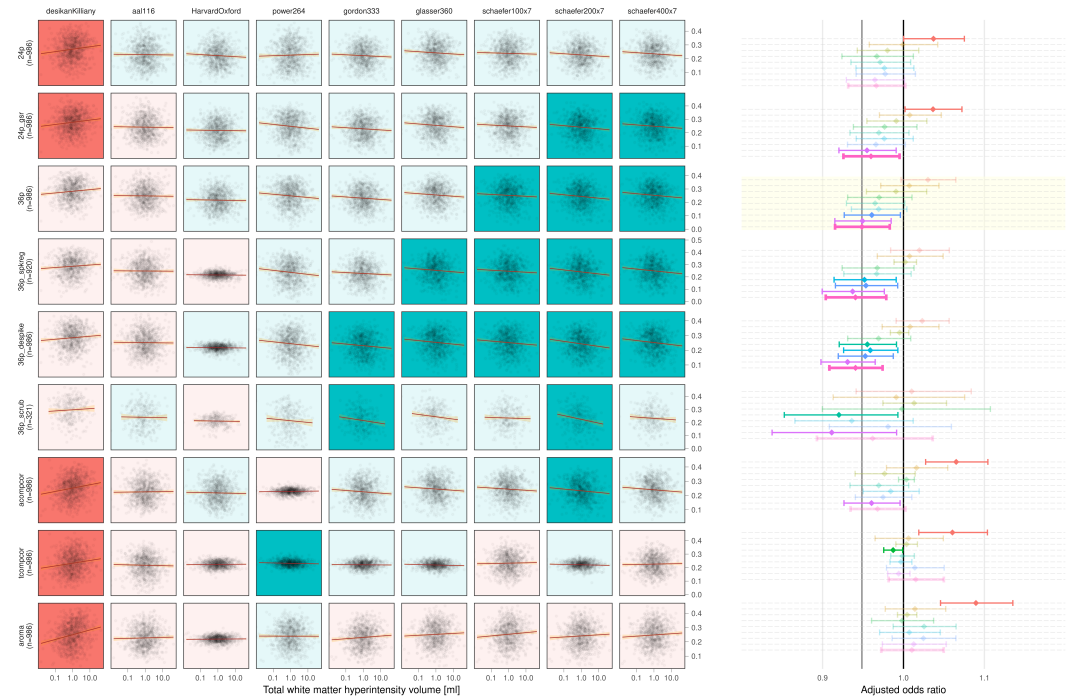


Figure 3. On the left, scatter plots of average fractional occupancies in high-occupancy states against WMH volume on a logarithmic scale (base 10 for easier visualization) for different combinations of confound regression strategies and brain parcellations. Linear regression lines indicate the direction of the unadjusted association between $\log(\text{WMH})$ and occupancy. Background color of individual panels indicates the direction of the association after adjustment for age, sex and zero WMH volume (green, negative; red, positive). A pale background indicates that the association between $\log(\text{WMH})$ and average occupancy is not statistically different from zero. On the right, the same information is shown using point estimates and 95 % confidence intervals for the adjusted odds ratio of the association.

252 performed previously using the BIANCA/LOCATE approach (Rimmele et al., 2022) and re-
253 sults are included in this preregistration (`./derivatives/WMH/cSVD_all.csv`). Functional
254 MRI data and clinical measures of executive dysfunction (TMT-B scores) have not been
255 analyzed by the author. Analysis of the data will begin immediately after acceptance-in-
256 principle of the stage 1 submission of the registered report is obtained. Submission of
257 the full manuscript (stage 2) is planned two months later.

258 Acknowledgment

259 This preprint was created using the LaPreprint template (<https://github.com/roaldarbol/lapreprint>) by Mikkel Roald-Arbøl .

261 References

- 262 Arbuthnott, Katherine and Janis Frank (2000). "Trail making test, part B as a measure of
263 executive control: validation using a set-switching paradigm". In: *Journal of clinical and*
264 *experimental neuropsychology* 22.4, pp. 518–528.
- 265 Behzadi, Yashar et al. (2007). "A component based noise correction method (CompCor)
266 for BOLD and perfusion based fMRI". In: *Neuroimage* 37.1, pp. 90–101.
- 267 Bos, Daniel et al. (2018). "Cerebral small vessel disease and the risk of dementia: A sys-
268 tematic review and meta-analysis of population-based evidence". en. In: *Alzheimers.*
269 *Dement.* 14.11, pp. 1482–1492.
- 270 Cannistraro, Rocco J et al. (2019). "CNS small vessel disease: A clinical review". en. In: *Neu-*
271 *rology* 92.24, pp. 1146–1156.
- 272 Ceric, Rastko, Adon FG Rosen, et al. (2018). "Mitigating head motion artifact in functional
273 connectivity MRI". In: *Nature protocols* 13.12, pp. 2801–2826.
- 274 Ceric, Rastko, Daniel H Wolf, et al. (2017). "Benchmarking of participant-level confound
275 regression strategies for the control of motion artifact in studies of functional con-
276 nectivity". en. In: *Neuroimage* 154, pp. 174–187.
- 277 Cornblath, Eli J et al. (2020). "Temporal sequences of brain activity at rest are constrained
278 by white matter structure and modulated by cognitive demands". en. In: *Commun Biol*
279 3.1, p. 261.
- 280 Cox, Robert W (1996). "AFNI: software for analysis and visualization of functional mag-
281 netic resonance neuroimages". In: *Computers and Biomedical research* 29.3, pp. 162–
282 173.

- 283 Das, Alvin S et al. (2019). "Asymptomatic Cerebral Small Vessel Disease: Insights from
284 Population-Based Studies". en. In: *J. Stroke Cerebrovasc. Dis.* 21.2, pp. 121–138.
- 285 Desikan, Rahul S et al. (2006). "An automated labeling system for subdividing the human
286 cerebral cortex on MRI scans into gyral based regions of interest". In: *Neuroimage* 31.3,
287 pp. 968–980.
- 288 Dey, Ayan K et al. (2016). "Pathoconnectomics of cognitive impairment in small vessel
289 disease: A systematic review". en. In: *Alzheimers. Dement.* 12.7, pp. 831–845.
- 290 Esteban, Oscar et al. (2019). "fMRIprep: a robust preprocessing pipeline for functional
291 MRI". en. In: *Nat. Methods* 16.1, pp. 111–116.
- 292 Frey, Benedikt M et al. (2021). "White matter integrity and structural brain network topol-
293 ogy in cerebral small vessel disease: The Hamburg city health study". en. In: *Hum. Brain*
294 *Mapp.* 42.5, pp. 1406–1415.
- 295 Friston, Karl J et al. (1996). "Movement-related effects in fMRI time-series". In: *Magnetic*
296 *resonance in medicine* 35.3, pp. 346–355.
- 297 Gesierich, Benno et al. (2020). "Alterations and test-retest reliability of functional connec-
298 tivity network measures in cerebral small vessel disease". en. In: *Hum. Brain Mapp.*
299 41.10, pp. 2629–2641.
- 300 Glasser, Matthew F et al. (2016). "A multi-modal parcellation of human cerebral cortex".
301 en. In: *Nature* 536.7615, pp. 171–178.
- 302 Gordon, Evan M et al. (2016). "Generation and Evaluation of a Cortical Area Parcellation
303 from Resting-State Correlations". en. In: *Cereb. Cortex* 26.1, pp. 288–303.
- 304 Griffanti, Ludovica, Mark Jenkinson, et al. (2018). "Classification and characterization of
305 periventricular and deep white matter hyperintensities on MRI: A study in older adults".
306 en. In: *Neuroimage* 170, pp. 174–181.
- 307 Griffanti, Ludovica, Giovanna Zamboni, et al. (2016). "BIANCA (Brain Intensity AbNormal-
308 ity Classification Algorithm): A new tool for automated segmentation of white matter
309 hyperintensities". en. In: *Neuroimage* 141, pp. 191–205.
- 310 Jagodzinski, Annika et al. (2020). "Rationale and Design of the Hamburg City Health Study".
311 en. In: *Eur. J. Epidemiol.* 35.2, pp. 169–181.
- 312 Laumann, Timothy O, Evan M Gordon, et al. (2015). "Functional system and areal organi-
313 zation of a highly sampled individual human brain". In: *Neuron* 87.3, pp. 657–670.
- 314 Laumann, Timothy O and Abraham Z Snyder (2021). "Brain activity is not only for thinking".
315 In: *Current Opinion in Behavioral Sciences* 40, pp. 130–136.

- ³¹⁶ Laumann, Timothy O, Abraham Z Snyder, et al. (2017). "On the stability of BOLD fMRI
³¹⁷ correlations". In: *Cerebral cortex* 27.10, pp. 4719–4732.
- ³¹⁸ Lawrence, Andrew J, Ai Wern Chung, et al. (2014). "Structural network efficiency is as-
³¹⁹ sociated with cognitive impairment in small-vessel disease". en. In: *Neurology* 83.4,
³²⁰ pp. 304–311.
- ³²¹ Lawrence, Andrew J, Daniel J Tozer, et al. (2018). "A comparison of functional and trac-
³²² tography based networks in cerebral small vessel disease". en. In: *Neuroimage Clin* 18,
³²³ pp. 425–432.
- ³²⁴ Lawrence, Andrew J, Eva A Zeestraten, et al. (2018). "Longitudinal decline in structural
³²⁵ networks predicts dementia in cerebral small vessel disease". en. In: *Neurology* 90.21,
³²⁶ e1898–e1910.
- ³²⁷ Macey, Paul M et al. (2004). "A method for removal of global effects from fMRI time series".
³²⁸ In: *Neuroimage* 22.1, pp. 360–366.
- ³²⁹ Makris, Nikos et al. (2006). "Decreased volume of left and total anterior insular lobule in
³³⁰ schizophrenia". In: *Schizophrenia research* 83.2-3, pp. 155–171.
- ³³¹ Muschelli, John et al. (2014). "Reduction of motion-related artifacts in resting state fMRI
³³² using aCompCor". In: *Neuroimage* 96, pp. 22–35.
- ³³³ Petersen, Marvin et al. (2020). "Network Localisation of White Matter Damage in Cerebral
³³⁴ Small Vessel Disease". en. In: *Sci. Rep.* 10.1, p. 9210.
- ³³⁵ Power, Jonathan D, Alexander L Cohen, et al. (2011). "Functional network organization of
³³⁶ the human brain". en. In: *Neuron* 72.4, pp. 665–678.
- ³³⁷ Power, Jonathan D, Anish Mitra, et al. (2014). "Methods to detect, characterize, and re-
³³⁸ move motion artifact in resting state fMRI". In: *Neuroimage* 84, pp. 320–341.
- ³³⁹ Prins, Niels D et al. (2005). "Cerebral small-vessel disease and decline in information pro-
³⁴⁰ cessing speed, executive function and memory". en. In: *Brain* 128.Pt 9, pp. 2034–2041.
- ³⁴¹ Pruim, Raimon HR et al. (2015). "ICA-AROMA: A robust ICA-based strategy for removing
³⁴² motion artifacts from fMRI data". In: *Neuroimage* 112, pp. 267–277.
- ³⁴³ Reijmer, Yael D et al. (2016). "Small vessel disease and cognitive impairment: The rele-
³⁴⁴ vance of central network connections". en. In: *Hum. Brain Mapp.* 37.7, pp. 2446–2454.
- ³⁴⁵ Rimmele, David Leander et al. (2022). "Association of Carotid Plaque and Flow Velocity
³⁴⁶ With White Matter Integrity in a Middle-aged to Elderly Population". en. In: *Neurology*.

- ³⁴⁷ Satterthwaite, Theodore D et al. (2013). "An improved framework for confound regression and filtering for control of motion artifact in the preprocessing of resting-state functional connectivity data". In: *Neuroimage* 64, pp. 240–256.
- ³⁵⁰ Schaefer, Alexander et al. (2018). "Local-Global Parcellation of the Human Cerebral Cortex from Intrinsic Functional Connectivity MRI". en. In: *Cereb. Cortex* 28.9, pp. 3095–3114.
- ³⁵² Schlemm, Eckhard et al. (2022). "Equalization of Brain State Occupancy Accompanies Cognitive Impairment in Cerebral Small Vessel Disease". en. In: *Biol. Psychiatry* 92.7, pp. 592–602.
- ³⁵⁵ Schulz, Maximilian et al. (2021). "Functional connectivity changes in cerebral small vessel disease - a systematic review of the resting-state MRI literature". en. In: *BMC Med.* 19.1, p. 103.
- ³⁵⁸ Shen, Jun et al. (2020). "Network Efficiency Mediates the Relationship Between Vascular Burden and Cognitive Impairment: A Diffusion Tensor Imaging Study in UK Biobank". en. In: *Stroke* 51.6, pp. 1682–1689.
- ³⁶¹ Steegen, Sara et al. (2016). "Increasing Transparency Through a Multiverse Analysis". en. In: *Perspect. Psychol. Sci.* 11.5, pp. 702–712.
- ³⁶³ Sundaresan, Vaanathi et al. (2019). "Automated lesion segmentation with BIANCA: Impact of population-level features, classification algorithm and locally adaptive thresholding". en. In: *Neuroimage* 202, p. 116056.
- ³⁶⁶ Tombaugh, Tom N (2004). "Trail Making Test A and B: normative data stratified by age and education". en. In: *Arch. Clin. Neuropsychol.* 19.2, pp. 203–214.
- ³⁶⁸ Tuladhar, Anil M, Ewoud van Dijk, et al. (2016). "Structural network connectivity and cognition in cerebral small vessel disease". en. In: *Hum. Brain Mapp.* 37.1, pp. 300–310.
- ³⁷⁰ Tuladhar, Anil M, Jonathan Tay, et al. (2020). "Structural network changes in cerebral small vessel disease". en. In: *J. Neurol. Neurosurg. Psychiatry* 91.2, pp. 196–203.
- ³⁷² Tzourio-Mazoyer, Nathalie et al. (2002). "Automated anatomical labeling of activations in SPM using a macroscopic anatomical parcellation of the MNI MRI single-subject brain". In: *Neuroimage* 15.1, pp. 273–289.
- ³⁷⁵ Vidaurre, Diego et al. (2018). "Discovering dynamic brain networks from big data in rest and task". en. In: *Neuroimage* 180.Pt B, pp. 646–656.
- ³⁷⁷ Wardlaw, Joanna M, Colin Smith, and Martin Dichgans (2013). "Mechanisms of sporadic cerebral small vessel disease: insights from neuroimaging". en. In: *Lancet Neurol.* 12.5, pp. 483–497.

- ³⁸⁰ Wardlaw, Joanna M, Eric E Smith, et al. (2013). "Neuroimaging standards for research
³⁸¹ into small vessel disease and its contribution to ageing and neurodegeneration". en.
³⁸² In: *Lancet Neurol.* 12.8, pp. 822–838.
- ³⁸³ Wardlaw, Joanna M, Maria C Valdés Hernández, and Susana Muñoz-Maniega (2015). "What
³⁸⁴ are white matter hyperintensities made of? Relevance to vascular cognitive impair-
³⁸⁵ ment". en. In: *J. Am. Heart Assoc.* 4.6, p. 001140.
- ³⁸⁶ Xu, Yuanhang et al. (2021). "Altered Dynamic Functional Connectivity in Subcortical Is-
³⁸⁷ chemic Vascular Disease With Cognitive Impairment". en. In: *Front. Aging Neurosci.* 13,
³⁸⁸ p. 758137.
- ³⁸⁹ Yeo, B T Thomas et al. (2011). "The organization of the human cerebral cortex estimated
³⁹⁰ by intrinsic functional connectivity". en. In: *J. Neurophysiol.* 106.3, pp. 1125–1165.
- ³⁹¹ Yin, Wenwen et al. (2022). "The Clustering Analysis of Time Properties in Patients With
³⁹² Cerebral Small Vessel Disease: A Dynamic Connectivity Study". en. In: *Front. Neurol.*
³⁹³ 13, p. 913241.